

Year of publication 2013

Mahuteau-Betzer F., Piguel S. (2013 Jun 12)

Synthesis and evaluation of photophysical properties of Series of π -conjugated oxazole dyes*Tetrahedron Letters* : 54 : 3188-3193 : DOI : <https://doi.org/10.1016/j.tetlet.2013.04.037>**Summary**

Incorporation of π -conjugated spacers at the 2 or 5 position of a 2,5-disubstituted aryloxazole led to new series of fluorescent dyes. They show emissions from visible to 700nm along with significant Stokes shift up to 208nm and a strong solvatochromic fluorescence. These compounds are easily accessible in one step through direct C-H bond functionalization.

Eric Quiniou, Paul Guichard, David Perahia, Sergio Marco, Liliane Mouawad (2013 May 7)

An atomistic view of microtubule stabilization by GTP.*Structure (London, England : 1993)* : 21 : 833-843 : DOI : [10.1016/j.str.2013.03.009](https://doi.org/10.1016/j.str.2013.03.009)**Summary**

A microtubule is a dynamic system formed of $\alpha\beta$ -tubulins. The presence of nonhydrolyzable guanosine-5'-triphosphate (GTP)/guanosine diphosphate (GDP) on the β -tubulins provokes microtubule polymerization/depolymerization. Despite the large number of experimental studies of this dynamical process, its mechanism is still unclear. To provide insights into this mechanism we studied the first depolymerization steps of GDP/GTP-bound microtubules by normal-mode analysis with the all-atom model. We also constructed a depolymerizing microtubule and compared it to cryo-electron microscopy tomograms (cryo-ET). The results show that during depolymerization, the protofilaments not only curve but twist to weaken their lateral interactions. These interactions are stabilized by GTP, but not evenly. Not all of the interface residues are of equal importance: five of them, belonging to the H2-S3 loop, play a special role; acting as a lock whose key is the γ -phosphate of GTP. Sequence alignments of several tubulins confirm the importance of these residues.

Rosa M Suárez, Franciane Chevot, Andrea Cavagnino, Nicolas Saettel, François Radvanyi, Sandrine Piguel, Isabelle Bernard-Pierrot, Véronique Stoven, Michel Legraverend (2013 Mar 1)

Inhibitors of the TAM subfamily of tyrosine kinases: synthesis and biological evaluation.*European journal of medicinal chemistry* : 2-25 : DOI : [10.1016/j.ejmech.2012.06.005](https://doi.org/10.1016/j.ejmech.2012.06.005)**Summary**

The TAM subfamily of Receptor **Tyrosine** Kinases (RTKs) contains three human proteins of therapeutical interest, Axl, Mer, and Tyro3. Our goal was to design a type II inhibitor specific for this family, i.e. able to interact with the **allosteric** pocket and with the hinge region of

the [kinase](#). We report the synthesis of several series of [purine](#) analogues of BMS-777607. The structural diversity of the designed inhibitors was expected to modify the interactions formed in the [binding site](#) and consequently to modulate their selectivity profiles. The most potent inhibitor **6g** exhibits K_d s of 39, 42, 65 and 200 nM against Axl, Mer, Met and Tyro3 respectively. Analysis of the affinity of **6g** for active and inactive forms of Abl1, an RTK protein that does not belong to the TAM subfamily, together with the binding modes of **6g** predicted by docking studies, indicates that **6g** displays some selectivity for the TAM family and may act as a type II inhibitor.

Year of publication 2012

Ada Collura, Laetitia Marisa, Diletta Trojan, Olivier Buhard, Anaïs Lagrange, Arnaud Saget, Marianne Bombléd, Patricia Méchighel, Mira Ayadi, Martine Muleris, Aurélien de Reynies, Magali Svrcek, Jean-François Fléjou, Jean-Claude Florent, Florence Mahuteau-Betzer, Anne-Marie Faussat, Alex Duval (2012 Sep 26)

Extensive characterization of sphere models established from colorectal cancer cell lines.

Cellular and molecular life sciences : CMLS : 2 : 729-42 : [DOI : 10.1007/s00018-012-1160-9](https://doi.org/10.1007/s00018-012-1160-9)

Summary

Links between cancer and stem cells have been proposed for many years. As the cancer stem cell (CSC) theory became widely studied, new methods were developed to culture and expand cancer cells with conserved determinants of "stemness". These cells show increased ability to grow in suspension as spheres in serum-free medium supplemented with growth factors and chemicals. The physiological relevance of this phenomenon in established cancer cell lines remains unclear. Cell lines have traditionally been used to explore tumor biology and serve as preclinical models for the screening of potential therapeutic agents. Here, we grew cell-forming spheres (CFS) from 25 established colorectal cancer cell lines. The molecular and cellular characteristics of CFS were compared to the bulk of tumor cells. CFS could be isolated from 72 % of the cell lines. Both CFS and their parental CRC cell lines were highly tumorigenic. Compared to their parental cells, they showed similar expression of putative CSC markers. The ability of CRC cells to grow as CFS was greatly enhanced by prior treatment with 5-fluorouracil. At the molecular level, CFS and parental CRC cells showed identical gene mutations and very similar genomic profiles, although microarray analysis revealed changes in CFS gene expression that were independent of DNA copy-number. We identified a CFS gene expression signature common to CFS from all CRC cell lines, which was predictive of disease relapse in CRC patients. In conclusion, CFS models derived from CRC cell lines possess interesting phenotypic features that may have clinical relevance for drug resistance and disease relapse.

Chevot F., Vabre R., Piguel S., Legraverend M. (2012 Apr 11)

Palladium-Catalyzed Amidation and Amination of 8-Iodopurine

European Journal of Organic Chemistry : 2012 : 2889-2893 : [DOI : 10.1002/ejoc.201200168](https://doi.org/10.1002/ejoc.201200168)

Summary

The synthesis of 8-amido- and 8-aminopurines by a single palladium-catalyzed protocol is reported. The method proceeds efficiently and tolerates a wide range of amides and amines as coupling partners, including aryl, alkyl, sulfone, and acetal amides, as well as deactivated m- and p-nitroanilines. In this way, a library of new 6,8,9-trisubstituted purines has been synthesized.

Year of publication 2011

Markhaba Tukenova, Catherine Guibout, Mike Hawkins, Eric Quiniou, Abddedahir Mousannif, Hélène Pacquement, David Winter, André Bridier, Dimitri Lefkopoulos, Odile Oberlin, Ibrahima Diallo, Florent de Vathaire (2011 Jun 1)

Radiation therapy and late mortality from second sarcoma, carcinoma, and hematological malignancies after a solid cancer in childhood.

International journal of radiation oncology, biology, physics : 80 : 339-346 : DOI :

[10.1016/j.ijrobp.2010.02.004](https://doi.org/10.1016/j.ijrobp.2010.02.004)

Summary

PURPOSE:

To compare patterns of long-term deaths due to secondary carcinomas, sarcomas, and hematological malignancies occurring after childhood cancer in a cohort of patients followed over a median of 28 years.

METHODS AND MATERIALS:

The study included 4,230 patients treated at eight institutions, who were at least 5-year survivors of a first cancer, representing 105,670 person-years of observation. Complete clinical, chemotherapeutic, and radiotherapeutic data were recorded, and the integral radiation dose was estimated for 2,701 of the 2,948 patients who had received radiotherapy. The integral dose was estimated for the volume inside the beam edges. The causes of death obtained from death certificates were validated.

RESULTS:

In total, 134 events were due to second malignant neoplasm(s) (SMN). We found that the standardized mortality ratio decreased with increasing follow-up for second carcinomas and sarcomas, whereas the absolute excess risk (AER) increased for a second carcinoma but decreased for second sarcomas. There was no clear variation in SMN and AER for hematological malignancies. We found a significant dose-response relationship between the radiation dose received and the mortality rate due to a second sarcoma and carcinoma. The risk of death due to carcinoma and sarcoma as SMN was 5.2-fold and 12.5-fold higher, respectively, in patients who had received a radiation dose exceeding 150 joules.

CONCLUSIONS:

Among patients who had received radiotherapy, only those having received the highest integral radiation dose actually had a higher risk of dying of a second carcinoma or sarcoma

Vabre R., Chevot F., Legraverend M., Piguel S. (2011 Jan 1)

Microwave-Assisted Pd/Cu-Catalyzed C-8 Direct Alkenylation of Purines and Related Azoles: An Alternative Access to 6,8,9-Trisubstituted Purines

The Journal of Organic Chemistry : 76 : 9542-9547 : [DOI : 10.1021/jo201893h](https://doi.org/10.1021/jo201893h)

Summary

An efficient microwave-assisted palladium/copper mediated C-8 direct alkenylation of purines with styryl bromides has been developed. The method is regioselective, functional group tolerant, rapid, and compatible with other related azoles. Combined with subsequent nucleophilic substitution, it provides an easy access to new 6,8,9-trisubstituted purines.

Year of publication 2010

Allard Aurore, Haddy Nadia, Le Deley Marie-Cécile, Rubino Carole, Lassalle Mathilde, Samsaldin Akthar, Quiniou Eric, Chompret Agnès, Lefkopoulos Dimitri, Diallo Ibrahima, De Vathaire Florent (2010 Dec 1)

Role of radiation dose in the risk of secondary leukemia after a solid tumor in childhood treated between 1980 and 1999.

International journal of radiation oncology, biology, physics : 78 : 1474-1482 : [DOI : 10.1016/j.ijrobp.2009.09.032](https://doi.org/10.1016/j.ijrobp.2009.09.032)

Summary

Purpose

The purpose of this study was to estimate the risk of secondary leukemia as a function of radiation dose, taking into account heterogeneous radiation dose distribution.

Methods and Materials

We analyzed a case-control study that investigated the risk of secondary leukemia and myelodysplasia after a solid tumor in childhood; it included 61 patients with leukemia matched with 196 controls. Complete clinical, chemotherapy, and radiotherapy histories were recorded for each patient in the study. Average radiation dose to each of seven bone marrow components for each patient was incorporated into the models, and corresponding risks were summed up. Conditional maximum likelihood methods were used to estimate risk parameters.

Results

Whatever the model, we failed to evidence a role for the radiation dose to active bone marrow in the risk of later leukemia, myelodysplasia, or myeloproliferative syndrome, when adjusting for epipodophyllotoxin and anthracycline doses. This result was confirmed when fitting models that included total dose of radiation delivered during radiotherapy, when fitting models taking into account dose per fraction, and when restricting the analysis to acute myeloid leukemia.

Conclusions

In contrast to results found in similar studies that included children treated before the use of epipodophyllotoxins, this study failed to show a role for radiotherapy in the risk of secondary leukemia after childhood cancer in children treated between 1980 and 1999. This discrepancy was probably due to a competitive mechanism between these two carcinogens.

Pacheco Berciano B., Lebrequier S., Besselièvre F., Piguel S. (2010 Sep 1)

1,1-Dibromo-1-alkenes as Valuable Partners in the Copper-Catalyzed Direct Alkynylation of Azoles

Organic Letters : 12 : 4038-4041 : [DOI : 10.1021/ol1016433](https://doi.org/10.1021/ol1016433)

Summary

The copper-catalyzed direct alkynylation of azoles with 1,1-dibromo-1-alkenes as electrophiles is described. These easily accessible substrates are a useful addition to the field of direct alkynylations in an efficient and functional group tolerant reaction to provide a straightforward entry to diverse alkynyl heterocycles.

Markhaba Tukenova, Ibrahima Diallo, Mike Hawkins, Catherine Guibout, Eric Quiniou, Hélène Pacquement, Frederic Dhermain, Akhtar Shamsaldin, Odile Oberlin, Florent de Vathaire (2010 Mar 5)

Long-term mortality from second malignant neoplasms in 5-year survivors of solid childhood tumors: temporal pattern of risk according to type of treatment.

Cancer epidemiology, biomarkers & prevention : a publication of the American Association for Cancer Research, cosponsored by the American Society of Preventive Oncology : 19 : 707-715 : [DOI : 10.1158/1055-9965.EPI-09-1156](https://doi.org/10.1158/1055-9965.EPI-09-1156)

Summary

BACKGROUND:

The temporal pattern in mortality from late second malignant neoplasms in solid childhood cancer survivors, according to the type of treatment, has not been investigated in detail.

METHODS:

We studied 4,230 5-year survivors of solid childhood cancer diagnosed between 1942 and 1986 in France and the United Kingdom. Complete clinical, chemotherapy, and radiotherapy data were recorded and the integral radiation dose was estimated for 2,701 of the 2,948 patients who had received radiotherapy.

RESULTS:

After a median follow-up of 28 years, 134 fatal events were due to second malignancies, compared with the 13.3 expected from the general France-UK population rates. The standardized mortality ratio was of a similar magnitude after radiotherapy alone and

chemotherapy alone and higher after both treatments. The standardized mortality ratio decreased with follow-up, whereas the absolute excess risk increased significantly over a period of at least 25 years after the first cancer. This temporal pattern was similar after chemotherapy alone, radiotherapy alone, or both treatments. We observed a similar long-term temporal pattern among survivors who had died of a second malignant neoplasm of the gastrointestinal tract and breast. Survivors who had received a higher integral radiation dose during radiotherapy were at a particularly high risk, as well as those who had received alkylating agents and epipodophyllotoxins.

CONCLUSIONS:

Five-year survivors of childhood cancer run a high long-term mortality risk for all types of second malignant neoplasms whatever the treatment received and require careful long-term screening well beyond 25 years after the diagnosis.

Year of publication 2009

François Besselièvre, Sandrine Piguel (2009 Dec 7)

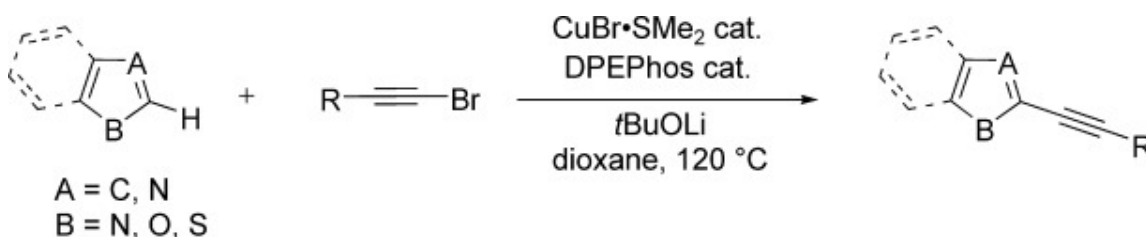
Copper as a powerful catalyst in the direct alkylation of azoles.

Angewandte Chemie (International ed. in English) : 48 : 9553-9556 : DOI :

[10.1002/anie.200904776](https://doi.org/10.1002/anie.200904776)

Summary

Copper-bottomed catalysis! The direct alkylation of azoles through a copper-based C—H bond activation, using alkynylbromides as the coupling partner, has been developed (see scheme). The method is very rapid, is functional-group tolerant, and provides a straightforward entry to diverse alkynyl heterocycles that is complementary to the Sonogashira reaction.



François Besselièvre, Sabrina Lebrequier, Florence Mahuteau-Betzer, Sandrine Piguel (2009 Sep 3)

C-H Bond Activation: A Versatile Protocol for the Direct Arylation and Alkenylation of Oxazoles

Synthesis : 2009 : 3511-3518 : DOI : [10.1055/s-0029-1216987](https://doi.org/10.1055/s-0029-1216987)

Summary

The versatile palladium complex Pd(PPh₃)₄ catalyses both direct arylation and alkenylation of oxazoles efficiently. The method is regioselective and stereospecific with respect to bromoalkenes and tolerates a wide range of functional groups.

Ibrahima Diallo, Nadia Haddy, Elisabeth Adjadj, Akhtar Samand, Eric Quiniou, Jean Chavaudra, Iannis Alziar, Nathalie Perret, Sylvie Guérin, Dimitri Lefkopoulos, Florent de Vathaire (2009 Apr 24)

Frequency distribution of second solid cancer locations in relation to the irradiated volume among 115 patients treated for childhood cancer.

International journal of radiation oncology, biology, physics : 74 : 876-883 : [DOI :](#)

[10.1016/j.ijrobp.2009.01.040](https://doi.org/10.1016/j.ijrobp.2009.01.040)

Summary

PURPOSE:

To provide better estimates of the frequency distribution of second malignant neoplasm (SMN) sites in relation to previous irradiated volumes, and better estimates of the doses delivered to these sites during radiotherapy (RT) of the first malignant neoplasm (FMN).

METHODS AND MATERIALS:

The study focused on 115 patients who developed a solid SMN among a cohort of 4581 individuals. The homemade software package Dos_{EG} was used to estimate the radiation doses delivered to SMN sites during RT of the FMN. Three-dimensional geometry was used to evaluate the distances between the irradiated volume, for RT delivered to each FMN, and the site of the subsequent SMN.

RESULTS:

The spatial distribution of SMN relative to the irradiated volumes in our cohort was as follows: 12% in the central area of the irradiated volume, which corresponds to the planning target volume (PTV), 66% in the beam-bordering region (i.e., the area surrounding the PTV), and 22% in regions located more than 5 cm from the irradiated volume. At the SMN site, all dose levels ranging from almost zero to >75 Gy were represented. A peak SMN frequency of approximately 31% was identified in volumes that received <2.5 Gy.

CONCLUSION:

A greater volume of tissues receives low or intermediate doses in regions bordering the irradiated volume with modern multiple-beam RT arrangements. These results should be considered for risk-benefit evaluations of RT.

Liliane Mouawad, Adriana Isvoran, Eric Quiniou, Constantin T Craescu (2009 Jan 22)

What determines the degree of compactness of a calcium-binding protein?

The FEBS journal : 276 : 1082-1093 : DOI : [10.1111/j.1742-4658.2008.06851.x](https://doi.org/10.1111/j.1742-4658.2008.06851.x)

Summary

The EF-hand calcium-binding proteins may exist either in an extended or a compact conformation. This conformation is sometimes correlated with the function of the calcium-binding protein. For those proteins whose structure and function are known, calcium sensors are usually extended and calcium buffers compact; hence, there is interest in predicting the form of the protein starting from its sequence. In the present study, we used two different procedures: one that already exists in the literature, the sosuidumbbell algorithm, mainly based on the charges of the two EF-hand domains, and the other comprising a novel procedure that is based on linker average hydrophilicity. The linker consists of the residues that connect the domains. The two procedures were tested on 17 known-structure calcium-binding proteins and then applied to 59 unknown-structure centrins. The sosuidumbbell algorithm yielded the correct conformations for only 15 of the known-structure proteins and predicted that all centrins should be in a closed form. The linker average hydrophilicity procedure discriminated well between all the extended and non-extended forms of the known-structure calcium-binding proteins, and its prediction concerning centrins reflected well their phylogenetic classification. The linker average hydrophilicity criterion is a simple and powerful means to discriminate between extended and non-extended forms of calcium-binding proteins. What is remarkable is that only a few residues that constitute the linker (between 2 and 20 in our tested sample of proteins) are responsible for the form of the calcium-binding protein, showing that this form is mainly governed by short-range interactions.

Year of publication 2008

Besselièvre F., Piguel S., Mahuteau-Betzer F., Grierson D.S. (2008 Aug 23)

Stereoselective Direct Copper-Catalyzed Alkenylation of Oxazoles with Bromoalkenes

Organic Letters : 10 : 4029-4032 : DOI : [10.1021/ol801512q](https://doi.org/10.1021/ol801512q)

Summary

A copper-catalyzed direct alkenylation of oxazoles with bromoalkenes has been developed. The method is both regio- and stereoselective and tolerates a variety of functional groups. A wide range of 2-*E*-vinyl-substituted oxazoles were obtained in high yields including the highly fluorescent alkaloid annuloline.